Published as:
Al-Lazki, A., Seber, D., Sandvol, E., Turkelli, N., Mohamad, R., and Barazangi, M., 2003. Tomographic Pn velocity and anisotropy structure beneath the Anatolian plateau (eastern Turkey) and the surrounding regions, *Geophys. Res. Lett.*, 30(24).

Tomographic Pn velocity and anisotropy structure beneath the Anatolian plateau (eastern Turkey) and the surrounding regions

Ali I. Al-Lazki[1*], Dogan Seber[1], Eric Sandvol[2], Niyazi Turkelli[3], Randa Mohamad[4], and Muawia Barazangi[1]

[1]Institute for the Study of the Continents, Cornell University, Ithaca, NY 14853
[2]Department of Geological Sciences, University of Missouri, Columbia, MO 65211
[3]Department of Geophysics, Kandilli Observatory and Earthquake Research Institute, Bogazici University, Istanbul, Turkey
[4]Syrian National Seismological Center, General Establishment of Geology and Mineral Resources, Damascus, Syria

Abstract. We use Pn phase travel time residuals to invert for mantle lid velocity and anisotropy beneath northern Arabia-eastern Anatolia continent-continent collision zone. The primary phase data were obtained from the temporary 29-station broadband PASSCAL array of the Eastern Turkey Seismic Experiment. These data were supplemented by phase data from available stations of the Turkish National Seismic Network, the Syrian National Seismic Network, the Iranian Long Period Array, and other stations around the southern Caspian Sea. In addition, we used carefully selected catalog data from the International Seismological Centre and the National Earthquake Information Center bulletins. Our results show that low (< 8 km/s) to very low (< 7.8 km/s) Pn velocity zones underlie the Anatolian plateau, the Caucasus, and northwestern Iran. Such low velocities are used to infer the presence of partially molten to absent mantle lid beneath these regions. In contrast, we observed a high Pn velocity zone

[*] Now at the Department of Earth Sciences, College of Science, P.O. Box 36, Postal Code 123, Alkhod, Sultanate of Oman.

beneath northern Arabia directly south of the Bitlis-Zagros suture indicating the presence of a stable Arabian mantle lid. This sharp velocity contrast across the suture zone suggests that Arabia is not underthrusting beneath the Anatolian plateau and that the surface suture extends down to the uppermost mantle.

Pn anisotropy orientations within a single plate (e.g. Anatolia plate) show a higher degree of lateral variation compared to Pn velocity. Areas of coherent Pn anisotropy orientations are observed to continue across major fault zones such as the EAF zone.

Introduction

This study focuses on the seismic structure of the continent-continent collision zone between the Arabian and Eurasian plates and the resultant Anatolian-Iranian plateau (Figure 1). Crustal processes at the Arabian-Eurasian convergent boundary and the nearby regions received extensive analysis [e.g., *Dewey et al.*, 1986; *Reilinger et al.*, 1997]. However, the state of the mantle lithosphere and lithospheric dynamics of this young continent-continent collision zone are still debated [e.g., *McKenzie*, 1972; *Rotstein and Kafka*, 1982; *Dewey et al.*, 1986].

The tectonic history of the region is complex. A two-phase extension episode in Late Eocene and Early Pliocene [*Hempton*, 1987] initiated the split of the Arabian plate from the African plate along the Red Sea and the Gulf of Aqaba regions. Arabia's continued northward motion and further separation from the African plate along the Dead Sea Fault (DSF) in the Miocene/Pliocene resulted in the reorganization of relative plate motions in the Anatolian Plateau [*Bozkurt*, 2001]. In Early Pliocene, this resulted in the westward extrusion of the Anatolian plate along the North Anatolian Fault (NAF) and the East Anatolian Fault (EAF) zones [*McKenzie*, 1972; *Sengor and Yilmaz*, 1981; *Sengor et* *al.*, 1985]. Farther north, the Lesser and Greater Caucasus regions which are believed to partially accommodate the Arabian plate northward motion [*Philip et al.*, 2001] are undergoing thrust and strike-slip deformation.

Terminal suturing of the Arabian and Eurasian plates along the Bitlis Suture (BS) is thought to have happened in the Middle Miocene [*Yilmaz*, 1993]. The Arabian-Eurasian collision is associated with extensive volcanism in eastern Anatolia, starting in the Late Miocene and continuing to historical times [*Keskin et al.*, 1998; *Yilmaz*, 1990]. The source of this volcanism is possibly derived from the lower portion of the lithospheric mantle [*Pearce et al.*, 1990]. GPS data [*Reilinger et al.*, 1997] have shown that the Anatolian plate is escaping to the west and that there is horizontal shortening across eastern Anatolia. The contribution of the mantle lid to convergence dynamics across the collision zone and the extent of Arabia's underthrusting beneath Eurasia are still not well-understood. This study aims at providing additional constraints for the models of the upper mantle dynamics in the region. Our results provide a much higher resolution Pn velocity model with anisotropy that significantly improves an earlier Pn velocity model of *Hearn and Ni* [1994] beneath the Anatolia-Arabia continent-continent collision zone and its surroundings.

Data and Inversion Method

We utilized two Pn phase data sets in this study. The fewer, but high quality data are obtained by manually reading 7,414 Pn phases from 29 PASSCAL broadband stations of the Eastern Turkey Seismic Experiment (ETSE), 5 short period stations of the Turkish National Seismic Network, 20 short period stations of the Syrian National Seismic Network, 5 broadband stations in the southern Caspian region, and 5 stations of the

Iranian Long Period Array (ILPA) located in northern Iran (Figure 1). The uncertainty of the Pn phase readings is less than one second. To include these data in our inversion we required a minimum of 10 different events per station and a minimum of 5 stations recording a single event. The larger quantity, but probably less reliable data were obtained from the existing seismic catalogues of the International Seismological Centre (ISC) and the National Earthquake Information Center (NEIC) to provide ray coverage where the high quality data were sparse. In this case, we used strict data selection criteria to select Pn phase data from these catalogues. We screened phase data for potential location errors by using a maximum azimuthal gap between stations of 150^o, a minimum of 20 recording stations per event, and less than 10 seconds of location residuals for each event. A total of about 51,000 Pn phase data were then used in the Pn tomography inversion for the area covering 30^o to 55^o E and 30^o to 45^o N.

A tomography method developed by *Hearn* [1996] is used to invert for Pn wave velocity and anisotropy, as well as station and event delays. This method uses a least squares algorithm [*Paige and Saunders*, 1982] to iteratively solve for all event-station pairs to obtain slowness, anisotropy, and station and event delays. The method includes damping parameters on both velocity and anisotropy to regularize solution and reduce noise artifacts. P-wave travel time residuals (<10 s) from sources at 1.8^o to 16^o were used to invert for uppermost mantle velocity and anisotropy models at a $1/6^o$ cell size, which is much smaller than cell size ($1/4^o$x$1/4^o$) used by Hearn and Ni, 1994 in Pn velocity inversion. A straight line fit for the initial travel time residuals versus distance gave an apparent Pn velocity of 8 km/s for the study area. In this tomography inversion we assumed a crustal thickness of 35 km and a crustal velocity average of 6.2 km/s". Figure 1 shows seismic stations atop hit counts map for the study region.

Tomography Results

A broad zone of low (< 8 km/s) Pn velocity underlies northwestern Iran, Turkey, and the Caucasus region. Within this broad low velocity anomaly, pockets of very low (< 7.8 km/s) Pn velocity zones are observed in the Caucasus and eastern Anatolia (Figure 2a). On the other hand, high Pn velocities underlie most of northern Arabia, the Caspian Sea and Azerbaijan (eastern Greater Caucasus), the Black Sea, and northeastern Mediterranean Sea (Figure 2a). In addition, smaller zones with high Pn velocity are observed in areas in northwestern Iran, central Anatolia plate, and central Greater Caucasus (Figure 2a).

To test the resolution of our tomographic inversion and the reliability of the anomalies obtained (Figure 2a) we constructed a synthetic checkerboard model with alternating high and low velocities in $2^{o}x2^{o}$ cells. We added 1 second random noise to the synthetic travel times obtained from the checkerboard model. We used the same inversion parameters and earthquake and station distributions identical to the observed data to invert for the synthetic travel time anomalies (Figure 2b). The checkerboard anomalies in most of the study area are well resolved except for moderate smearing observed in northwestern Iran, the Caspian Sea, the Black Sea, and southern parts of northern Arabia (Figure 2b). In these regions smearing is more severe on the anisotropy resolution indicating that anisotropy orientations in these regions are not reliable, while areas of better resolved anisotropy orientations coincided with very well resolved velocity checkers (Figure 2b).

The event and station distributions in the study area are not uniform. While the ETSE and Syrian National Seismic Network (SNSN) stations provide very dense coverage in a small region, additional stations cover other parts of the region sparsely. In order to take advantage of the high density station coverage of the ETSE and SNSN and to obtain a higher resolution Pn image along the collision zone we conducted a special, focused study by only using data from the ETSE and SNSN. All phase picks for these stations came from digital data and read by the authors. This data set is clearly higher quality than the bulletin phase database in this region. Using this higher quality subset of our data set we obtained a detailed Pn velocity image at this segment of the collision zone (Figure 3a). We used the earlier model cell size ($1/6^o$) and used a smaller damping value (100 rather than 1000) on this data set since the noise in this subset of data set is much lower. This resulted in a clearly defined northernmost boundary of the Arabian plate along the EAF and the BS zones (Figure 3a). Figure 3b shows checkerboard test results obtained for this subset of data. In this case we used 1.5^ox1.5^o sized checkerboard anomalies. The synthetic results show that the resolution is high along the BS and the EAF zones (the area of interest) and at the junction of the North and East Antolian Fault zones.

Observed anisotropy orientations and amplitude simultaneously inverted with Pn velocity show a higher degree of lateral variability compared to Pn velocity (Figure 4). Anisotropy orientations within the Anatolian plate and along the NAF vary from predominantly E-W in the center to more N-S in the western parts of Turkey (Figure 4). Zones of NE-SW anisotropy orientations surround the easternmost portion of the NAF zone, and along the Lesser Caucasus region. The latter two NE-SW anisotropy orientations spatially correlate with zones of very low Pn velocities, and show anisotropy magnitudes that are larger than their surroundings (Figure 4).

Discussion and Conclusions

The geodynamic model governing the accommodation of the Arabian plate's northward motion has been the subject of an ongoing debate [*McKenzie*, 1972; *Rotstein and Kafka*, 1982; *Dewey et al.*, 1986]. In this study, we presented evidence on the state of the lithospheric mantle beneath this young continent-continent collision zone. Geologic data from eastern Anatolia and the Caucasus indicate that the latest stage of collision related volcanism started in the Late Miocene and continued until historical times [*Keskin et al.*, 1998; *Yilmaz*, 1990]. Upper mantle instability in this region is also evidenced by young calc-alkaline and alkaline volcanism (Fig. 2a) [*Innocenti et al.*, 1976; *Pearce et al.*, 1990]. At the present time, we observe a broad scale low and smaller scale very low Pn velocity anomalies beneath northwestern Iran, Eastern Anatolian plateau, the Caucasus region, and most of the Anatolian plate (Figure 2a). Comparably, Sn wave propagation anomalies in this region also show high attenuation beneath the Anatolian plate, the Anatolian plateau, and the Caucasus region [*Gok et al.*, 2000; *Sandvol et al.*, 2001]. These results are also consistent with mantle lid instability interpretation beneath the Eurasian side of the collision (i.e., northwestern Iran, eastern Anatolia, the Caucasus, and Anatolia plate). We interpret that partially molten to eroded mantle lid exists in regions underlain by very low Pn velocity anomalies, such as the easternmost portion of the NAF, and the Lesser and western Greater Caucasus regions (Figure 2a). The very low Pn velocity may even be interpreted to indicate the complete absence of mantle lid in these regions, and that asthenospheric material is directly located beneath the crust. This interpretation rules out the earlier proposed idea of mantle thickening of the lithosphere [*Dewey et al.*, 1986] beneath the Anatolian plateau and the Caucasus region. If there were ever a lithospheric thickening in these regions, either delamination or convective removal of the thickened mantle lithosphere might have eliminated the thick lithosphere.

Our results invalidate the idea of Arabian plate subduction or underthrusting beneath the eastern Anatolian plateau as suggested by *Rotstein and Kafka* [1982]. Stable mantle lid regions as identified by high Pn velocities underlie only the northernmost portion of the Arabian plate. This high velocity sharply stops along the Bitlis suture zone (Figure 2a). Using a higher resolution subset of data we show that the northern bounds of Arabia's high mantle lid velocities follow the western BS and the EAF lines relatively well (Figure 3a). It is worthy to note that an isolated small positive anomaly occurs in northwestern Iran. This anomaly located in an area with obvious velocity smearing (Figure 2b) may not entirely be explained by NW-SE smearing artifact (see Figure 2b), because both ends (NW and SE) of the positive anomaly are occupied by low negative velocity anomalies. This suggests that the positive anomaly may be caused by a genuine response of a stable upper mantle beneath this part of northwestern Iran.

In continental settings anisotropy orientations are commonly described to mimic regional tectonic trends [e.g., *Kendall*, 2000]. Compared to Pn velocity, mantle lid Pn anisotropy shows relatively more variations within a single plate (e.g., Anatolian plate) or along a single tectonic boundary (e.g., NAF). Observed Pn anisotropy orientations do not seem to follow the tectonic trends. The more sudden anisotropy variations in eastern Turkey and the Caucasus region may possibly reflect more complex deformation processes in this region.

Acknowledgments.

The authors are grateful for the help and assistance of our colleagues E. Zor, R. Gok, T. Bekler, R. Kay, S. Kuleli, K. Al-Damegh, C. Brindisi, and F. Gomez. We are thankful for the help of the federal and local governments of Turkey. This research is supported by the National Science Foundation (Grant No. EAR-9804780) and Bogazici University Research Fund (Grant No. 99T206).

References

Bozkurt, E., Neotectonics of Turkey - a synthesis, *Geodinamica Acta : The Europian Journal of Geodynamics*, *14* (1-3), 3-30, 2001.

Dewey, J.F., M.R. Hempton, W.S.F. Kidd, F. Saroglu, and A.M.C. Sengor, Shortening of continental lithosphere: the neotectonics of Eastern Anatolia - a young collision zone, in *Collision Tectonics*, edited by M.P. Coward, and A.C. Ries, pp. 3-36, Geological Society Special Publication, 1986.

Gok, R., N. Turkelli, E. Sandvol, D. Seber, and M. barazangi, Regional wave propagation in Turkey and surrounding regions, *Geophysical Research Letters*, *27* (3), 429-432, 2000.

Hearn, T.M., Anisotropic Pn tomography in the western United States, *Journal of Geophysical Research*, *101* (B4), 8403-8414, 1996.

Hearn, T.M., and J.F. Ni, Pn velocities beneath continental collision zones: the Turkish-Iranian Plateau, *Geophysical Journal International*, *117*, 273-283, 1994.

Hempton, M.R., Constraints on Arabian plate motion and extensional history of the Red Sea, *Tectonics*, *6* (5), 687-705, 1987.

Innocenti, P., R. Mazzuoli, G. Pasquare, F.R.D. Brozolo, and L. Villare, Evolution of the volcanism in the area of interaction between Arabian, Anatolian and Iranian plates (Lake Van, eastern Turkey), *J. Volcan. Geotherm. Res*, *1*, 103-112, 1976.

Kendall, J.-M., Seismic anisotropy in the boundary layers of the mantle, in *Deep Earth Interior: Mineral physics and tomography from the atomic to the global scale*, edited by S.-i. Karato, A.M. Forte, R.C. Liebermann, G. Masters, and L. Stixrude, pp. 115-159, American Geophysical Union, 2000.

Keskin, M., J.A. Pearce, and J.G. Mitchell, Volcano-stratigraphy and geochemistry of collision-related volcanism on the Erzurum-Kars Plateau, northeastern Turkey, *Journal of Volcanology and Geothermal Research*, *85*, 355-404, 1998.

McKenzie, D., Active tectonics of the Mediterranean region, *Geophysical Journal of the Royal Astronomical Society*, *30*, 109-185, 1972.

Paige, C.C., and M.A. Saunders, LSQR: Sparse linear equations and least squares problem, *ACM Transactions on Mathematical Software*, *8* (2), 195-209, 1982.

Pearce, J.A., J.F. Bender, S.E. Delong, W.S.F. Kidd, P.J. Low, Y. Guner, F. Saroglee, Y. Yilmaz, S. Moorboath, and J.G. Mitchell, Gensis of collisional volcanism in eastern Anatolia, Turkey, *J. Volc. geotherm. Res.*, *44*, 189-229, 1990.

Philip, H., A. Avagyan, A. Karakhanian, J.-F. Ritz, and S. Rebai, Estimating slip rates and recurrence intervals for strong earthquake along an intracontinental fault: example of the Pambak-Sevan-Sunik fault (Armenia), *Tectonophysics*, *343*, 205-232, 2001.

Reilinger, R.E., S.C. McClusky, M.B. Oral, R.W. King, M.N. Toksoz, A.A. Barka, I. Kinik, O. Lenk, and I. Sanli, Global Positioning System measurements of present-day crustal movements in the Arabia-Africa-Eurasia plate collision zone, *Journal of Geophysical Research*, *102* (B5), 9983-9999, 1997.

Rotstein, Y., and A.L. Kafka, Seismotectonics of the southern boundary of Anatolia, eastern Mediterranean region; subduction, collision, and arc jumping, *Journal of Geophysical Research*, *87* (9), 7694-7706, 1982.

Sandvol, E., K. Al-Damegh, A. Calvert, D. Seber, M. Barazangi, R. Mohamad, R. Gok, N. Turkelli, and C. Gurbuz, Tomographic imaging of Lg and Sn propagation in the Middle East, *Pure and Applied Geophysics*, *158*, 1121-1163, 2001.

Sengor, A.M.C., N. Gorur, and F. Sargolu, Strike-slip faulting and related basin formation in zones of tectonic escape: Turkey as a case study, in *Strike-slip faulting and basin formation*, edited by K.T. Biddle, and N. Christie-Blick, pp. 227-264, Society of Econ. Paleontol. Mineral. Special Publication, 1985.

Sengor, A.M.C., and Y. Yilmaz, Tethyan evolution of Turkey: a plate tectonic approach, *Tectonophysics*, *75*, 181-241, 1981.

Yilmaz, Y., Comparison of young volcanic associations of western and eastern Anatolia formed under a compressional regime: a review, *Journal of Volcanology and Geothermal Research*, *44*, 69-87, 1990.

Yilmaz, Y., New evidence and model on the evolution of the southeast Anatolian orogen, *Geological Society of America Bulletin*, *105* (2), 251-271, 1993.

Figure Captions

Figure 1. Simplified tectonic boundaries (black lines) of northern Arabian and Eurasian plates atop hit counts base-map for every 1/6^o cell size. 1 = White triangles are Eastern Turkey Seismic Experiment (ETSE) stations, and black triangles are Syrian National Seismic Network (SNSN) stations; white hexagons are Turkish National Seismic Network stations, black hexagons are temporary stations of the southern Caspian experiment; white stars are the temporary station of the Iranian Long Period Array (ILPA); and open triangles are other local stations obtained from the ISC catalouge. 2 = Thrust, and 3 = strike-slip fault boundaries. BS = Bitlis Suture and ZS = Zagros Suture, GC = Greater Caucasus, LC = Lesser Caucasus, NAF = North Anatolian Fault, EAF = East Anatolian Fault, DSF = Dead Sea Fault.

Figure 2. **(a)** A map showing inverted tomographic image of Pn velocity of the study area. 1= Neogene/Quaternary volcanoes, 2= Thrust boundary, and 3= Strike-slip boundary. **(b)** Checkerboard test results for 2^{o}x2^o cells inverted using the same station and event distribution used in the velocity and anisotropy model shown in Figure 2a.

Figure 3. **(a)** A map showing our tomographic image of Pn velocity using only the data picked and read by the authors. The upper bounds of high Pn velocity zone along the EAF and the eastern BS are used to define the northern extent of the Arabian plate boundary. **(b)** A map showing 1.5°x1.5° checkerboard test results inverted using the same stations and events distribution for Figure 3a. The best resolution is along the EAF, eastern BS zones, and at the intersection zone between the EAF and NAF zones. Symbols are as in Figure 2.

Figure 4. A map showing Pn anisotropy inverted simultaneously with the velocity model. See Figure 2a for text abbreviation in map.

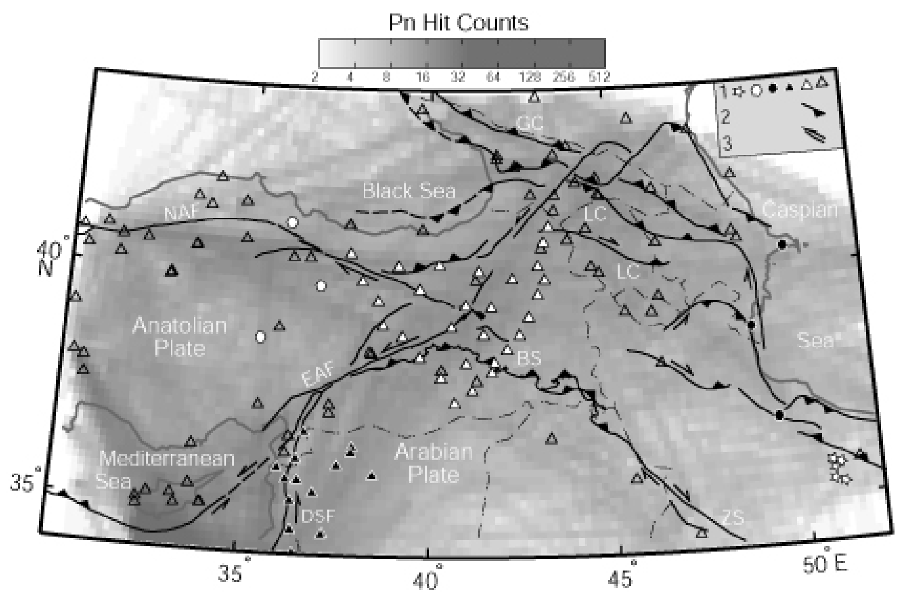

Figure 1

Figure 2a

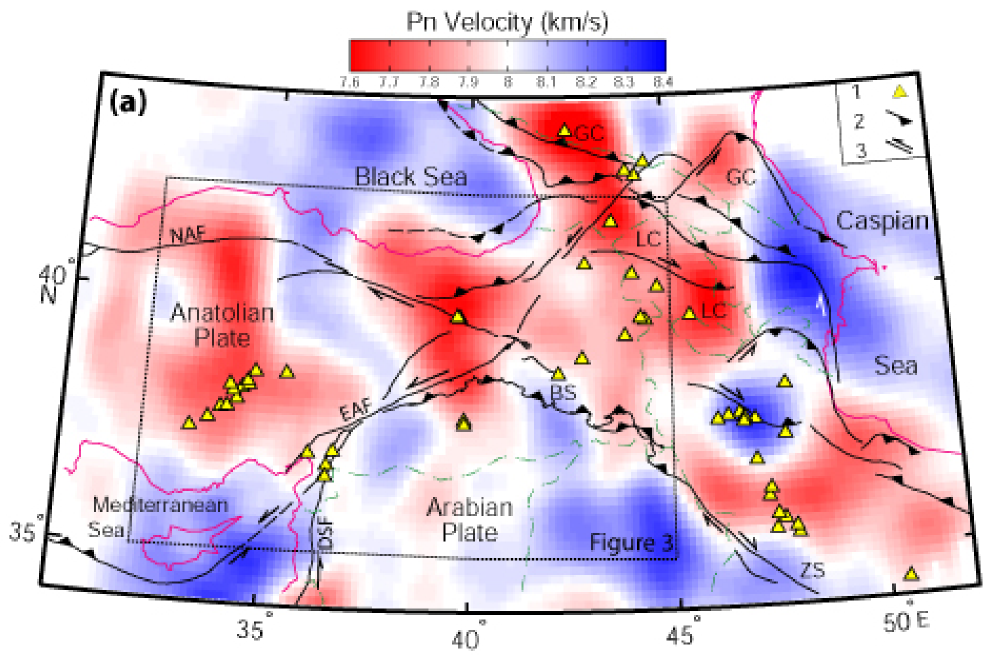

Figure 2b

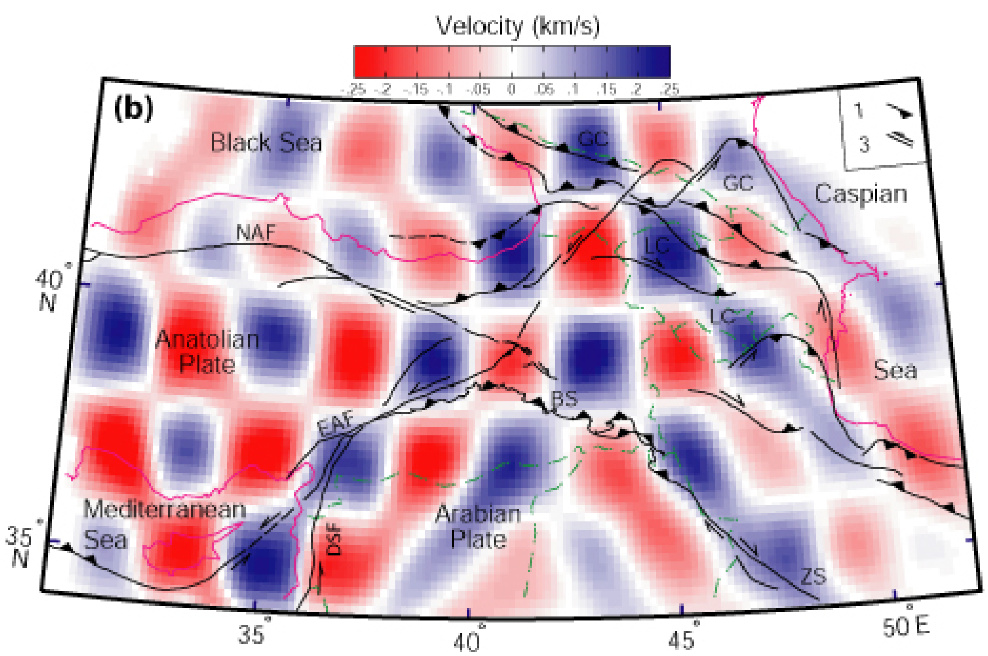

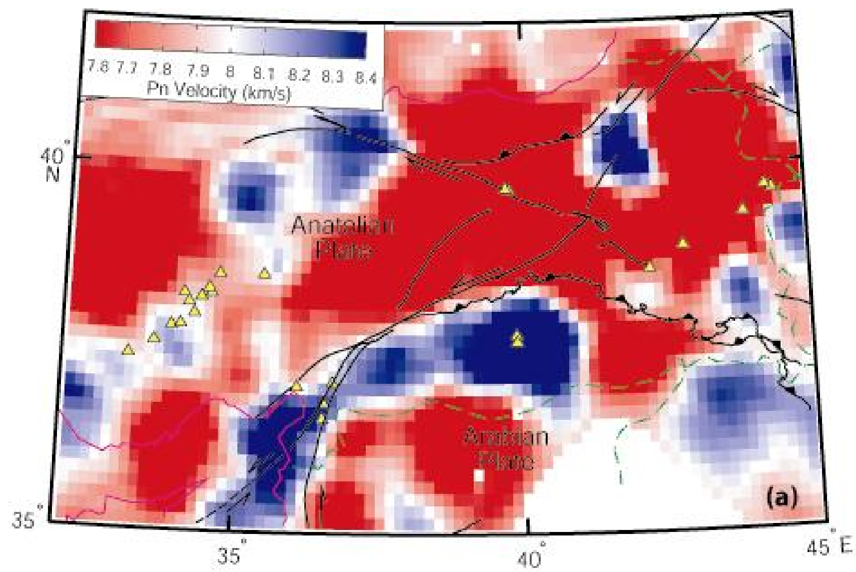

Figure 3a

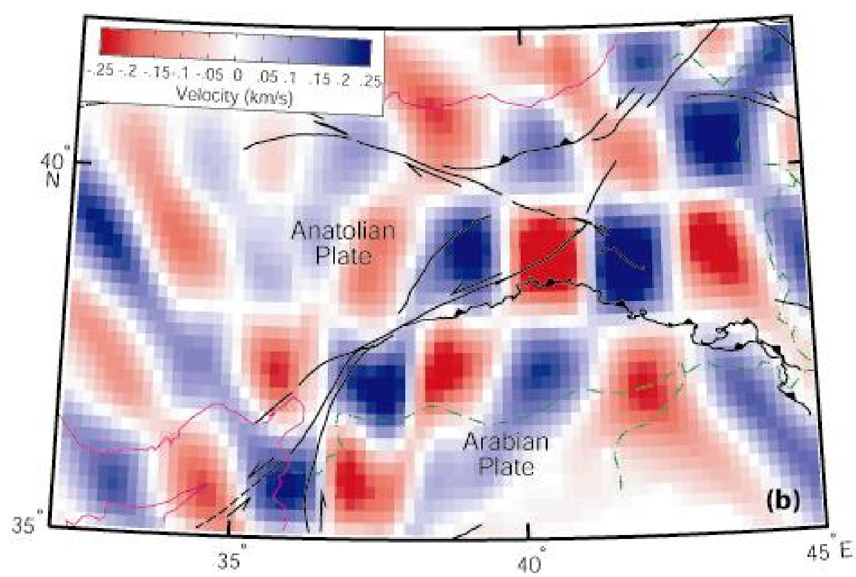

Figure 3b

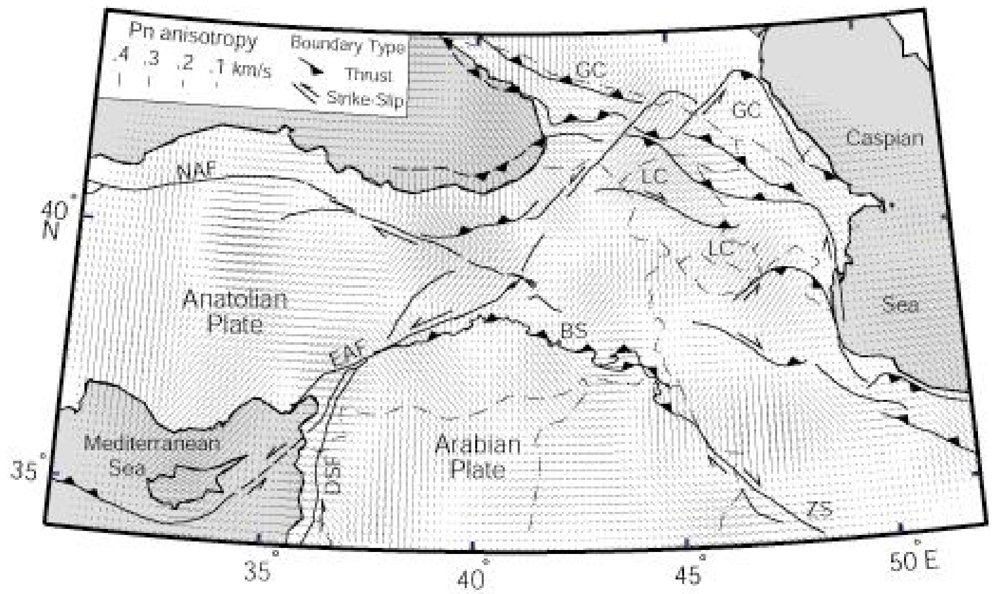
Pn anisotropy
.4 .3 .2 .1 km/s
Boundary Type
Thrust
Strike-Slip
GC
GC
Caspian
NAF
LC
LC
40° N
Anatolian Plate
Sea
BS
EAF
Mediterranean Sea
Arabian Plate
DSF
35°
ZS
35°
40°
45°
50° E

Figure 4